https://doi.org/10.5194/bg-2023-174
Preprint. Discussion started: 29 September 2023

Biogeosciences Discussions
Open Access
EGU

Crystalline Iron Oxides Stimulate Methanogenesis Under Sulfate Reducing Conditions in the Terrestrial Subsurface

Brandon C. Enalls[1], Mon Oo Yee[1], Amrita Bhattacharyya[2,3], Kristine Cabugao Grace[1], Sara Gushgari-Doyle[1], Terry C. Hazen[4,5,6], Romy Chakraborty[1#]

[1]Department of Ecology, Earth & Environmental Sciences Area, Lawrence Berkeley National Laboratory, Berkeley, California 94720, USA

[2]Department of Geochemistry, Earth & Environmental Sciences Area, Lawrence Berkeley National Laboratory, Berkeley, California 94720, USA

[3]Department of Chemistry, University of San Francisco, San Francisco, California 94117, USA

[4] Department of Earth and Planetary Sciences, University of Tennessee, Knoxville, Tennessee 37996, USA

[5]Genome Sciences Division, Oak Ridge National Lab, Oak Ridge, Tennessee 37830, USA

[6]Department of Civil and Environmental Engineering, University of Tennessee, Knoxville, Tennessee 37996, USA

Correspondence to: Romy Chakraborty (RChakraborty@lbl.gov)

https://doi.org/10.5194/bg-2023-174
Preprint. Discussion started: 29 September 2023

Abstract. Microbial methane production is intimately linked to the biogeochemical cycling of iron, sulfur, and carbon in sedimentary environments. Sulfate-reducing microbes often outcompete methanogens for shared substrates. However, in a prior study at our field site, the Oak Ridge Reservation Field Research Center (ORR FRC) in Oak Ridge, TN, we observed co-occurring sulfate reduction and methanogenesis at 100-150 cm depth where iron (Fe) oxides of varying crystallinities were also detected. Fe oxides are known to act as electron conduits for direct interspecies electron transport (DIET) between syntrophic partners and can connect the metabolisms of methanogens with syntrophic Fe-reducing microbes in nature. However, whether the nature of Fe oxides can influence electron transfer reactions between sulfate-reducing microbes and methanogens is less understood. In this study, we utilized a microbial community enriched from ORR FRC vadose zone sediment to demonstrate the effects of Fe oxides of varying crystallinities on sulfate reduction and methanogenesis. We hypothesized that more crystalline Fe oxides facilitate the co-existence of sulfate-reducers and methanogens. Communities enriched from subsurface sediments produced methane when amended with crystalline hematite but not when amended with the amorphous, short range-ordered (SRO) ferrihydrite. Furthermore, Fe reduction occurred only in incubations amended with SRO ferrihydrite, indicating how poorly crystalline Fe oxides potentially contribute to the dynamic redox nature of the subsurface sediments. Microbial communities enriched during these incubations were composed of several taxa commonly associated with iron and sulfate reduction, fermentation, and methanogenesis, consistent with our geochemical data. Overall, the results from this work deepen our understanding of the role of Fe oxides in extracellular electron transfer, thereby mediating anaerobic metabolisms in the terrestrial subsurface environment.

1 Introduction

In subsurface sedimentary environments, carbon cycling and methane emissions are intimately linked to other biogeochemical processes, including those related to the cycling of sulfur and iron (Jørgensen et al., 2019; Jørgensen and Kasten, 2006). Subsurface biogeochemical cycling is a poorly understood component of global carbon cycle, particularly in respect to the processes that mediate methanogenesis. It is critical to constrain both the biotic and abiotic processes that govern these complex ecological processes. When sulfate is present in anoxic zones within sediments, sulfate-reducing bacteria (SRB) often outcompete methane-producing archaea (methanogens), resulting in distinct zones of sulfate reduction and methanogenesis (Claypool and Kaplan, 1974). This metabolic advantage of SRB is due to the higher affinity of their enzymes for shared substrates and to the thermodynamic favorability of sulfate reduction as compared to methanogenesis (Kristjansson et al., 1982; Schönheit et al., 1982). In addition, methanogens suffer from the toxicity effects of the reduced sulfur (S) compound, hydrogen sulfide, more acutely than SRB (Koster et al., 1986). Nonetheless, co-existence of the two groups has been observed in anaerobic environments and were explained by non-competitive substrate usage under high organic loading rates (Oremland and Polcin, 1982) or under low sulfate conditions (Ozuolmez et al., 2020). However, these specific conditions

https://doi.org/10.5194/bg-2023-174
Preprint. Discussion started: 29 September 2023

do not fully account for the broadly observed co-existence of the two dominant anaerobic metabolisms, warranting further investigation into other factors that may also impact this phenomenon in the complex terrestrial subsurface.

A previous study at our field site, the Oak Ridge Reservation Field Research Center (ORR FRC) in Oak Ridge, TN, USA indicated the coincidence of methane production and sulfate reduction. Specifically, high methane production rates coinciding with sulfate reduction were reported in the vadose zone (100-150 cm depth) of the subsurface sediments (Moon et al., 2020). Both SRB and methanogens can participate in the syntrophic degradation of organic matter in sedimentary environments, where SRB catalyze the breakdown of volatile fatty acids and other more complex organic substrates into simple substrates, such as acetate, carbon dioxide, and hydrogen gas, which can then either be used for methanogenesis (Dworkin et al., 2006; Nozhevnikova et al., 2020) or further metabolized to continued sulfate reduction (Thauer et al., 2007). Given the kinetic and thermodynamic advantages that SRB have over methanogens, the coexistence of these two metabolisms is unexpected under the environmental conditions at our field site, possibly challenging what we know about subsurface biogeochemistry.

Notably, high concentrations of crystalline Fe oxides were also detected at our field site in the same zone as concomitant sulfate reduction and methanogenesis (Moon et al., 2020). The redox potential of the Fe(III)–Fe(II) redox couple lies between the redox potentials of the major C, N, O or S redox couples (Michael Madigan et al., 2019), and therefore, the presence of Fe oxides adds a new layer of complexity to C and S cycling. Moreover, Fe oxides show distinct electrochemical properties depending on their crystal structures; for example, crystalline hematite (α-Fe_2O_3) is semiconductive whereas amorphous ferrihydrite is insulating (Cornell and Schwertmann, 2003; Xu and Schoonen, 2000). Several laboratory-based studies have shown that these Fe oxides can connect syntrophic metabolisms between microbial partners by serving as conduits that mediate direct interspecies electron transport (DIET) (Kato et al., 2012; Park et al., 2018). Many Fe(II)-oxidizing and Fe(III)-reducing bacteria are metabolically flexible as well, which helps them adapt to the availability of electron donors and acceptors that mediate environmental redox reactions. Some of the studied mechanisms of electron transfer from microorganisms to Fe(III) minerals include direct contact between the bacterial cell and Fe(III) minerals, secretion of chelating agents to complex with Fe minerals, electrically conductive pili and multistep electron hopping via redox cofactors that are present in biofilms (Melton et al., 2014). While crystalline minerals such as hematite can promote microbially mediated electron transfer through conductive nanowires, short-range ordered (SRO) insulating Fe (oxy)hydroxides such as ferrihydrite are instrumental in interacting with chelating agents such as EDTA through reductive dissolution and co-precipitation (Mikutta et al., 2008; Weihe et al., 2019; Zhou et al., 2014). The provision of Fe oxides has additionally been shown to enhance rates of syntrophic methanogenesis in several studies using sediment-hosted microbial communities (Aromokeye et al., 2018, 2020; Rotaru et al., 2018; Zhang and Lu, 2016). However, these enrichments were performed using sulfate-free media, and as such the specific contributions of SRB were not investigated. Therefore, it remains unclear whether SRB participate in syntrophic methanogenesis via DIET using Fe oxide minerals as conduits for electron transfer.

We hypothesized that crystalline Fe oxides facilitate metabolic interactions between sulfate-reducers and methanogens in the ORR FRC vadose zone, allowing these microbes to coexist under conditions that typically result in

https://doi.org/10.5194/bg-2023-174
Preprint. Discussion started: 29 September 2023

competition for substrates. In this study, we use a microbial community enriched from ORR FRC vadose zone sediment to demonstrate the effects of Fe oxides of varying crystallinities on sulfate reduction and methanogenesis. In addition to the microbially mediated processes, abiotic reaction mechanisms were also investigated to untangle the biotic and abiotic controls for the reaction. The interplay of microbially-mediated and abiotic reactions in the biogeochemical Fe and S cycles helps us develop a better understanding of the role of Fe oxides and electron transfer reactions in anoxic zones within the terrestrial subsurface.

2 Materials and Methods

2.1 Sediment Collection

Sediments were collected from borehole EB271 in March 2017 near the S-3 pond at the Oak Ridge Reservation Field Research Center (ORR FRC) located within the Y-12 National Security Complex in Oak Ridge Tennessee, USA (see Watson et al., 2004 for more information on this site and Moon et al., 2020 for detailed location information and geochemical analysis of borehole EB271). Our inoculum was collected at a depth of 100-150 cm, the same depth where methane production, sulfate reduction, and the presence of Fe oxide minerals were previously reported (Moon et al., 2020). Sediments were frozen and stored at -80 °C upon collection for microbial and biogeochemical analyses.

2.2 Culture Conditions

A novel, custom mineral growth medium that mimics the geochemical conditions of the sampling location (sediment core EB271) at the ORR FRC was developed to replicate the field conditions as closely as possible and create environmentally relevant experimental conditions, which is hereafter referred to as the EB271 medium. Briefly, the EB271 mineral medium contained mineral salts, a selenite/tungstate solution (1 mL), a trace element solution (1 mL), L-cysteine as the reducing agent (0.6 g), N-[Tris(hydroxymethyl)methyl]-2-aminoethanesulfonic acid (TES, 2.292) and $NaHCO_3$ (2.5 g) as buffers, and 0.25 ml 0.1% w/v resazurin as an oxygenation indicator. The mineral salts were comprised of NH_4Cl (0.3 g), KH_2PO_4 (0.2 g), $MgCl_2$-$6H_2O$ (0.5 g), and $CaCl_2$-$2H_2O$ (0.015 g) per liter. The selenite/tungstate solution contained Na_2SeO_4-$6H_2O$ (0.0006 g) and Na_2WO_4-$5H_2O$ (0.0008 g) per liter. The trace elements solution contained HCl (0.01 ml 25% w/w), H_3BO_3 (0.006 g), NaOH (0.5 g), $MnCl_2$-$4H_2O$ (0.1 g), $CoCl_2$-$6H_2O$ (0.19 g), $ZnCl_2$ (0.07 g), $CuCl_2$-$2H_2O$ (2.0 mg), $NiCl_2$-$6H_2O$ (2.4 mg) Na_2MoO_4-$2H_2O$ (0.036 g), $FeSO_4$-$7H_2O$ (2 g) and $AlKSO_4$-$12H_2O$ (0.1 g) per liter. The vitamin solution contained d-biotin (2.0 mg), folic acid (2.0 mg), pyroxidine-HCl (10.0 mg), thiamine-HCl (5.0 mg), riboflavin (5.0 mg), nicotinic acid (5.0 mg), pantothenic acid (5 mg), vitamin B12 (0.1 mg), p-aminobenzoic acid (5.0 mg), and lipoic acid (5.0 mg) per liter.

To obtain a sediment-free microbial inoculum for our experimental incubations, a preconditioning enrichment of EB271 sediment was conducted in anoxic EB271 medium amended with 5 mM sodium butyrate and 10 mM sodium sulfate for approximately 6 months under a N_2:CO_2 (80:20) headspace. Butyrate was chosen as primary electron acceptor for this experiment as previous work showed that many simple carbon sources, including glucose or acetate, do not promote diverse

https://doi.org/10.5194/bg-2023-174
Preprint. Discussion started: 29 September 2023

communities of microbes from our field site (Wu et al., 2020). In addition, butyrate is known to stimulate syntrophic metabolisms under sulfate-reducing and methanogenic conditions (Struchtemeyer et al., 2011). We transferred this enrichment three times (two-month incubation intervals) at 10 % v/v inoculum prior to the start of our experimental incubations described in this work. All later experimental incubations using this enriched inoculum were also conducted using 5 mM sodium butyrate and 10 mM sodium sulfate maintained under an N_2:CO_2 (80:20) headspace and ran for ~ 3 months.

To test the influence of Fe(III) minerals in our incubations, hematite or ferrihydrite were added in concentrations of 1% w/v. Hematite comprised a majority of conductive minerals in sediment bore EB271 (Moon et al., 2020) and was chosen to mimic field conditions whereas ferrihydrite was chosen because of its reduced crystallinity and increased reactivity compared to hematite.

To better understand the microbial influences in our system, several sets of biotic control incubations were conducted where we inhibited the metabolisms of specific groups of microbes. Incubations were performed in parallel using either 5 mM 2-bromoethanesulfonate (BES) to inhibit methanogenesis (Goenrich et al., 2004) or 10 mM sodium molybdate to inhibit sulfate reduction (Taylor and Oremland, 1979). Incubations without the addition of minerals or metabolism inhibitors were conducted to serve as controls for the experimental treatments. Treatments with no added minerals or metabolism inhibitors served as controls for all incubation conditions (See Table 1 descriptions of experimental incubations and acronyms used to describe each treatment).

We also concurrently performed abiotic incubations containing no microbial inoculum with and without the presence of 10 mM sulfide to investigate abiotic influences on the geochemical dynamics of our systems (See Table 2 for descriptions of abiotic incubations and acronyms used to describe each treatment). All biotic and abiotic incubations were conducted in triplicate.

2.3 Geochemical Analyses

Samples for geochemical analyses were collected periodically throughout the incubation. Under sterile and anoxic conditions, 1 mL from the headspace was taken (while replacing headspace volume with 1 mL N_2:CO_2 gas) to measure methane using gas chromatography with a thermal conductivity detector with helium as the carrier gas (6890N Network GC System; Agilent Technologies; Santa Clara, CA, USA). Methane concentrations were calculated to account for changes in headspace volume due to regular sampling of the cultures. To quantify sulfate, butyrate, acetate, Fe(II), and dissolved sulfide, 1 mL of the culture was taken and sterilized with 0.2 µm PES filters prior to analysis. Sulfate, butyrate, and acetate were measured using ion chromatography (Dionex ICS 2100; Thermo Fisher Scientific; Waltham, MA, USA). Samples for Fe(II) quantification were acidified usinf 0.5 N HCl and quantified using a modified version of the ferrozine assay (Stookey, 1970) using a microplate reader (BioteK Epoch2; Agilent; Santa Clara, CA, USA). Dissolved sulfide quantification immediately fixed in 91 mM zinc acetate was determined using colorimetric analysis within a day of sampling using a modified microplate version of the Cline assay (Cline, 1969).

https://doi.org/10.5194/bg-2023-174
Preprint. Discussion started: 29 September 2023

2.4 X-ray Absorption Spectroscopy

Synchrotron-based X-ray absorption spectroscopy (XAS) was used to determine Fe and S speciation (oxidation state and chemical coordination environment). S and Fe K-edge X-ray absorption near-edge structure (XANES) and iron K-edge extended x-ray absorption fine structure (EXAFS) spectral analyses were conducted on beamline 4-3 at the Stanford Synchrotron Radiation Laboratory (SSRL), at Menlo Park, CA under ring operating conditions of 3 GeV with a current of 450 mA. Experiments were performed in pure helium to minimize absorption and scattering from the atmosphere. Samples were sealed on Teflon holders with Kapton tape to preserve the oxidation state of Fe and S to prevent any potential beam damage which might occur during data collection. A double crystal Si (220) monochromator with an unfocused beam was detuned 30% to reject harmonics affecting the primary beam. Pure elemental Fe foil was used for energy calibration for Fe at 7112 eV whereas thiosulfate ($S_2O_3^{2-}$) was used for energy calibration of S at 2472 eV. The Lytle detector was used to record the fluorescence spectra of EXAFS and XANES scans. Between 7 and 10 individual spectra were averaged for each sample. Fluorescence spectra were background subtracted and the atomic absorption was normalized to unity using Athena(Ravel and Newville, 2005).

2.5 16S Microbial Community Analyses

To examine changes in microbial community composition over time, two 2 mL aliquots of culture were collected from days 0 (T0), 36 (T4), and 87 (T8) from each vial containing live microbes and were centrifuged. The supernatants were decanted, and the pellets were frozen at -80 °C until extraction. Samples were extracted using the Qiagen DNeasy PowerLyzer PowerSoil Kit following the manufacturer's suggested protocol. Negative control samples were generated during each round of extractions to be included in the sequencing run.

Extracted genomic DNA was sent to Novogene Corporation, Inc. for quality control and subsequent sequencing with the Illumina MiSeq. Microbial community composition was analyzed by targeting the V4 region of the 16S gene with the 515F (5'-GTGCCAGCMGCCGCGGTAA-3') and 806R (5'-GGACTACHVGGGTWTCTAAT-3') primer pair (Caporaso et al., 2011) to generate 300 bp paired-end reads. A subset of samples were also sequenced using the archaeal specific 519F (5'-CAGCCGCCGCGGTAA-3') and 915R (5'-GTGCTCCCCCGCCAATTCCT-3') primer pair (Herfort et al., 2009; Casamayor et al., 2002). Sequences were analyzed via the Qiime2 paired-end read pipeline version 2022.2 (Bolyen et al., 2019). Representative sequences that were found in both the experimental and negative controls at a prevalence of 0.05 or higher were marked as contaminants and were removed from the experimental samples using the R package *decontam* (Davis et al., 2018). Sequences were taxonomically assigned using the Silva database release 138. Nonmetric multidimensional scaling (NMDS) indices and ordination ellipses drawn around the mean centroid (95% CI) were constructed using Bray Curtis dissimilarity metrics using the R package *vegan* (Dixon, 2003).

https://doi.org/10.5194/bg-2023-174
Preprint. Discussion started: 29 September 2023

3 Results and Discussion

3.1 Geochemical Analyses

We examined changes in the concentrations of analytes relevant to the metabolisms of interest (butyrate, acetate, sulfate, sulfide, methane, and Fe(II)) to determine whether the addition of either hematite or ferrihydrite to our cultures influenced the physiologies of our enriched microbial communities. Conditions S, SH, and SF represent treatments where no mineral or inhibitor were added (see Table 1 for information on treatments and all corresponding acronyms). Throughout the 87-day incubation period, we observed 4.3 ± 0.16 mM, 4.0 ± 0.3 mM, and 3.8 ± 0.5 mM butyrate consumed and 6.8 ± 2.5, 9.0 ± 2.1 mM, and 7.6 ± 6.4 mM sulfate reduced by these cultures, respectively (Fig. 1). In conditions S and SH, net 4.8 ± 0.4 mM and 1.7 ± 1.8 mM acetate and 3.7 ± 1.8 mM and 0.15 ± 0.023 mM aqueous sulfide were respectively produced. In condition SF, net 0.60 ± 0.45 mM acetate was consumed over 87 days with a peak aqueous acetate concentration of 8.8 ± 0.087 mM on day 17. We only detected methane production in condition SH, representing cultures that contained uninhibited microbes amended with hematite. We observed 3.3 ± 5.8 mM of methane produced over the duration of the incubation, suggesting that this more crystalline Fe oxide may be required for methanogenesis to occur in this system. We observed acid extractable Fe(II) accumulation in condition SF, peaking at 2.0 ± 2.4 mM on day 42. We were unable to detect any accumulation in any hematite-amended or mineral-free cultures.

We performed incubations using BES to inhibit methanogenesis and in these cultures (SB, SHB, and SFB), 4.6 ± 0.75, 4.0 ± 0.41, and 3.9 ± 0.40 mM butyrate was consumed and 7.6 ± 0.30, 7.3 ± 3.2, and 11 ± 0.66 mM sulfate was reduced, respectively, throughout the incubation period (Fig. 1). As expected, we did not observe methane accumulated in any BES treated culture. In conditions SB and SHB, net 5.0 ± 0.15 and 5.2 ± 2.2 mM acetate was produced, respectively. Cultures from SBF conditions produced net-zero acetate over the 87-day experiment with a maximum aqueous acetate concentration of 8.9 ± 0.80 mM on day 17. Fe(II) was only detected in condition SFB, peaking at 1.3 ± 0.90 mM on day 36.

In cultures where molybdate was added to inhibit sulfate reduction (conditions SM, SHM, SFM), there was no notable consumption of butyrate or sulfate nor was there production of sulfide or methane (Fig. 1). Ferrous iron peaked at 0.52 ± 0.15 mM on day 52 in condition SFM but was not detected in SM and SHM. Small amounts of acetate were produced in all sulfate reduction inhibited cultures, peaking at 2.9 ± 0.47 mM for condition SM, 2.5 ± 0.14 mM for condition SHM, and 2.9 ± 0.10 mM for condition SFM by day 17.

It is interesting to note that while we did not observe Fe(II) accumulation in our hematite treated conditions, we did ferrihydrite-amended cultures showed Fe(II) accumulation. This was likely due to increased crystallinity of hematite compared to ferrihydrite, rendering, it a more difficult electron acceptor for microbes to use (Schwertmann, 1991). This idea is supported by prior work showing decreased Fe reduction in the presence of hematite compared to less crystalline Fe oxides for both pure cultures (Li et al., 2006) and enrichments (Zhang et al., 2020) of Fe-reducing microbes. In addition, the rapid precipitation of new minerals upon reduction of hematite may have also occurred. For example, precipitation of crystalline spinels such as magnetite precipitated during incubation, may have underestimated Fe(II) production (Benner et al., 2002). We also observed

https://doi.org/10.5194/bg-2023-174
Preprint. Discussion started: 29 September 2023

decreases in Fe(II) concentrations towards the end of these incubations, due to the potential coprecipitation of Fe (oxy)hydroxides and Fe sulfides that is typically observed following the reductive dissolution of Fe oxides, especially in association with organic matter (Cornell and Schwertmann, 2003; Li et al., 2006; Neal et al., 2001). Finally, the observed accumulation of ferrous iron in condition SF may have also been due to increased rates of fermentative iron reduction, which would also be supported by faster butyrate consumption concurrent with higher peak acetate production at earlier time points when compared to conditions S and SH.

Control incubations where no microbial inoculum was added were performed to examine any abiotic changes in analyte concentrations in the medium (See Table 2 for description of control conditions). The observed some decreases in both butyrate and sulfate concentrations throughout the incubation period for all treatments was smaller in magnitude than the respective biotic incubations (Fig. S1), indicating that active microbial metabolisms were the primary driving factor for the changes in analyte concentrations. In condition CS, where no mineral was added, we observed a decrease of 6.36 ± 0.98 mM sulfide, which may be attributed to the introduction of oxygen during the sampling process. Sulfide depletion in conditions CHS and CFS was likely due to interactions between the added iron oxide minerals. Given the differences in reactivity versus hematite and ferrihydrite, it is not surprising that we observed total depletion of sulfide in condition CHS slowly over the first 52 days while no sulfide was able to accumulate in cultures from condition CFS due to rapid oxidization by ferrihydrite. We did not observe accumulation of acetate, methane, or Fe(II) in any of our control incubations. Overall, these control incubations provided context for the changes in analyte concentrations caused by active microbial metabolisms.

3.2 Iron and sulfur speciation under (a)biotic incubations during syntrophic butyrate degradation

Synchrotron-based XAS data provided critical molecular-scale insights on the coupled Fe-S redox chemistry during incubations in the presence and absence of BES and molybdate inhibitors as a function of altered mineral crystallinity (ferrihydrite being the amorphous or poorly crystalline and hematite being the crystalline mineral).Overall, Fe K-edge XANES data indicates that bulk Fe was in +3 oxidation state across all the experimental incubations tested both under biotic and abiotic conditions (Fig 2A). Subtle changes in the relative peak positions (lower and higher values indicating reduced and oxidized Fe species, respectively) together with spectral shapes and intensities in the XANES region among the different samples indicated that the relative proportions of Fe(II) and Fe(III) varied as a function of mineral crystallinity across the samples incubated with specific inhibitors. In the absence of inhibitors (conditions SH and SF), the maximum peak intensities for SF and SH occurred at ~7129.5 eV and ~7133 eV respectively, indicating that bulk Fe is in +3 oxidation state (O'Day et al., 2004). A similar trend is observed in BES treated cultures (SFB and SHB). When comparing molybdate incubated samples (conditions SHM and SFM), the average oxidation state of Fe is similar between these treatments.

In general, samples incubated with ferrihydrite exhibited the maximum differences in uninhibited and BES treated cultures (conditions SF and SFB), hinting at potential biotic Fe reduction promoted by amorphous ferrihydrite. This is also supported by observed changes in the coordination environment of Fe atoms (determined via EXAFS analysis) in samples from SF and SFB when compared to pristine ferrihydrite (Fig. S2). Samples from hematite amended conditions (SH, SHB,

https://doi.org/10.5194/bg-2023-174
Preprint. Discussion started: 29 September 2023

SHM) maintained similar EXAFS patterns when compared to pristine hematite, suggesting Fe atoms in hematite remained relatively untouched during incubation. For molybdate treated samples, the distinct pre-edge peak at ~ 7114.7 eV in SFM when compared to that of SHM indicated that Fe from the ferrihydrite treatment has a well-defined stable molecular geometry, despite ferrihydrite being the amorphous mineral (Fig. 2A). This finding is in accordance with literature data which shows that short-range ordered ferrihydrite-like minerals often are the controlling factors for mineral-organic matter stabilization and subsequent preservation in terrestrial ecosystems (Kleber et al., 2015).

To explore abiotic versus biotic reduction mechanisms, Fe XANES data were also collected on the abiotic incubations (CS, CFS and CHS) (Fig. 2A). The similarities in peak positions between our abiotic control incubations indicate that the mechanisms of iron reduction were predominantly biotic in nature.

Upon analysis of the sulfur speciation in our samples by S K-edge XANES (Fig. 2B), peaks at ~2482.7 eV in most of our samples indicated the presence of sulfate (S in +6 oxidation state, Prietzel et al., 2011). The absence of this peak in conditions SF, SHB, SFB indicate that sulfate was reduced into other sulfur speceis by SRB during these incubations. Peaks at ~2472.6 eV in a few treatments (CHS, CFS, SFB) were indicative of the presence of elemental sulfur (Prietzel et al., 2011), likely a product of reaction between dissolved sulfide and Fe oxide minerals (Poulton, 2003; Pyzik and Sommer, 1981; Yao and Millero, 1996). Additionally, the presence of sulfonate (S in +5 oxidation state) at ~ 2481.3 eV was observed across all treatments (Prietzel et al., 2011)), likely due to the use of TES buffer in the incubation medium. No sulfide species indicative of Fe sulfide minerals (~ 2470.7 eV for FeS and ~ 2471.3 eV for FeS_2,(Prietzel et al., 2011)) was observed, indicating that the bulk mineralogical speciation from hematite and ferrihydrite were retained during the incubations.

3.3 Microbial Community Composition

To examine how the addition of either hematite or ferrihydrite affected the composition of the microbial communities enriched in our experiment, the DNA from samples collected at day 0 (T0), day 36 (T4) and day 87 (T8) from all biotic incubations was extracted and the 16S rRNA gene was sequenced (Fig. 3).

A large proportion of the communities from our initial inoculum were strict or facultative anaerobic fermenters (Fig. 3, samples labeled T0). Organisms from the class Clostridia were the most abundant members of these communities, with ASVs matching to the genus *Lachnoclostridium*, spore forming anaerobes that produce acetate as their major fermentation product (Yutin and Galperin, 2013). Microorganisms within the Bacteroidia families Dysgonomonadaceae, Paludibacteraceae, or Prevotellaceae were also enriched and are known to be strict or facultative anaerobes capable of fermenting complex polysaccharides (Owusu-Agyeman et al., 2022; Parte et al., 2011; Ueki, 2006). Members of the Paludibacteraceae have previously been enriched in both microbial electrolysis cells and microbial fuel cells under anoxic conditions, suggesting their potential for extracellular electron transfer reactions and possible involvement in similar interactions with conductive minerals in sedimentary environments (Kim et al., 2011; Satinover et al., 2020). The only cultured genus of the Paludibacteraceae known to date is Paludibacter, which is known to produce propionate and acetate as major fermentation products (Ueki, 2006). Other fermenters that were enriched include *Lactobacillus* of the class Bacilli which were only found in the second replicate

https://doi.org/10.5194/bg-2023-174
Preprint. Discussion started: 29 September 2023

of this initial inoculum (sample T0S2). The high relative abundances of these fermentative organisms in our samples are not surprising given that our initial microbial communities were pre-conditioned for several subcultures anoxically using the fermentable substrate butyrate as a primary electron donor.

In addition to these fermenters, organisms from the classes Desulfotomaculia and Desulfitobacteria were also enriched in our T0 samples. ASVs from within the Desulfotomaculia matched to the genera *Desulfallus* and *Desulfurispora,* which are canonically known to engage in sulfate reduction, with the latter putatively thought to also engage in iron reduction (Kaksonen et al., 2007; Watanabe et al., 2020; Wen et al., 2018), as well the genus *Sporotomaculus,* another genus of anaerobic fermenters (Brauman et al., 1998). Within the Desulfitobacteria, members of the sulfate-reducing genus *Desulfosporosinus* (Hippe and Stackebrandt, 2015) were enriched, though some members of the genus are also known to engage in iron reduction (Hippe and Stackebrandt, 2015). The methanogenic archaeal class, Methanobacteria, was observed in T0S3. These ASVs matched to *Methanobacterium sp*., organisms known to engage in hydrogenotrophic methanogenesis.

Overall, the microbial communities making up the starting inoculum contained higher total observed ASVs and Shannon diversity indices compared to our experimental conditions (Fig. S3), suggesting that our communities became selectively structured throughout our incubations through decreases in species richness. Inverse Simpson indices (which incorporates both species richness and evenness) were largely similar between the starting inoculum and most of the experimental conditions. Higher Inverse Simpson indices were observed for several communities which exhibited greater evenness among observed ASVs, including communities collected at day 87 and provided molybdate as an inhibitor (T8SM, T8SHM, and T8SFM), as well as In the communities collected at day 37 and provided hematite and molybdate (T4SHM), suggesting that the addition of molybdite lead to changes in the relative abundances of the organisms enriched under these conditions.

Communities from incubations where no minerals were added contained many of the same organisms found in our initial inoculum (Fig. 3). Interestingly, shifts in the relative abundances of putative sulfate- and iron-reducing microbes occurred over time, where we observed greater representation of Desulfitobacteria in T4 samples and observed higher relative abundances of Desulfotomaculia in T8 samples. Methanobacteria were observed in varying abundances in these sets of incubations, except in those where methanogenesis was inhibited using BES (condition SB).

Organisms from the class Coriobacteria were also detected in all 'No Mineral' conditions, with ASVs matching to Actinobacteria OPB41. While transcriptomics and enzyme assays performed on uncultured group OPB41 representatives from marine sediments suggested the capacity for anaerobic sugar hydrolysis (Bird et al., 2019), two organisms from this group that have been isolated recently for the first time are confirmed to be either sulfur- or Fe-reducers (Khomyakova et al., 2022). Organisms from the class Negativicutes were also enriched during these incubations, with the majority of ASVs within this class matching to the acetogenic genus *Sporomusa sp*. While acetogens in general are known for their wide substrate utilization (Drake et al., 1997), *Sporomusa* are typically known to use a variety of substrates ranging from CO_2 (Breznak and Blum, 1991; Tremblay and Zhang, 2015) to sugars, methanol, and N-methylated compounds (Visser et al., 2016). Since the data reported in our study are the result of subcultured communities (at 10% v/v inoculum), it is possible that a portion of the energy driving

https://doi.org/10.5194/bg-2023-174
Preprint. Discussion started: 29 September 2023

the observed acetogenesis is from the subcultured incubation and the carbon may be derived from carryover organic carbon or CO_2, which was present in the serum bottle headspace. *Sporomusa sp*. were detected in higher relative abundances in incubations where either methanogens or sulfate-reducers were inhibited. Since methanogens and sulfate-reducers both generally have thermodynamic advantages over acetogens for shared substrates (Lever, 2012), it is likely acetogens were able to persist in higher abundance in these inhibited conditions because of reduced competition. This likely also explains the production of acetate in molybdate treated samples observed in our geochemical analyses (Fig. 1, panels SM, SHM, and SFM).

We used Bray Curtis analyses to statically measure dissimilarities in community composition between our experimental treatments and constructed NMDS plots to observe these differences. We observed little overlap between the ordination ellipses highlighting the "Initial" and "No Mineral" treatment groups (Fig. S4), suggesting the microbial communities from treatment groups were significantly different from each other. These results were supported by a p-value of 0.001 calculated from pairwise PERMANOVA analysis of Bray Curtis metrics between these two treatment groups (Table S1). The differences between these treatment groups are likely the result of selective structuring of the microbial communities during the incubation period, which is also corroborated by decreases in total observed ASVs and Shannon Diversity metrics between these groups as described earlier (Fig. S3).

The addition of Fe oxide minerals to the cultures also significantly impacted the composition of microbial communities. There was also little overlap in ordination ellipses between the "Initial" treatment and either the "Hematite" and "Ferrihydrite" treatments (Fig.S4), which was also supported by Pairwise PERMANOVA p-values of 0.001 between these treatment groups (Table S1). PERMANOVA analyses comparing the "No Mineral" treatment group with either the "Hematite" and "Ferrihydrite" treatments also resulted in p-values <0.05 (Table S1), despite visual overlap in ordination ellipses between these groups (Fig. S4). Interestingly, we did not detect significant differences between the "Hematite" and "Ferrihydrite" treatments, as the p-value for this pairwise PERMANOVA analysis was calculated to be 0.196. These data suggest that while the addition of an iron oxide to the incubation lead to distinct microbial communities, the type of iron oxide (whether it be hematite of ferrihydrite) did not seem to any specific differences in community composition.

Many of these mineral amended cultures, specifically those that were incubated with either BES or no added metabolism inhibitors (conditions SH, SHB, SF, and SFB), were largely dominated by Desulfitobacteriia (Fig. 3). The relative abundances of Desulfitobacteriia and Desulfotomaculia were greatly diminished in incubations where molybdate was added (conditions SHM and SFM). The inhibition of sulfate-reducing metabolisms through the addition of molybdate allowed for Clostridia to increase in relative abundance, making up the vast majority of these communities.

Organisms from the classes Bacteriodia and Anaerolineae were found in many of the samples collected from both hematite and ferrihydrite amended cultures at T8. ASVs within Anaerolineae matched to uncultured *Leptolinea*, *Pelolinea*, and *Levilinea*, organisms known to be anaerobic fermenters (Imachi et al., 2014; Yamada et al., 2006). Uncultured members of the Anaerolineae have also previously been enriched under iron reducing conditions. Organisms from the class Myxococcia were also observed in many of the ferrihydrite treated samples, with ASVs matching to the genus *Anaeromyxobacter,* members of which are known iron reducers (He and Sanford, 2003; Petrie et al., 2003). The higher reactivity of ferrihydrite likely

https://doi.org/10.5194/bg-2023-174
Preprint. Discussion started: 29 September 2023

allowed *Anaeromyxobacter* (and likely other Fe reducers) to reduce Fe at greater rates during these incubations. This is supported by detection of Fe(II) in both ferrozine assays (Fig. 1) as well Fe K-edge XANES analyses (Fig. 2A) performed on samples collected from this set of incubations.

We detected *Methanobacterium sp*., known for performing hydrogenotrophic methanogenesis (Boone, 2015), in varying abundances in a few cultures across many experimental conditions, despite only observing methane production in cultures amended with hematite and no metabolism inhibitors. Interestingly, we also only observed *Methanosarcina sp*. in low relative abundance in one hematite amended culture at one time point (T4SH1). *Methanosarcina* are known to engage in both DIET and in extracellular electron uptake reactions directly from cathodes (Rowe et al., 2019; Yee et al., 2019; Yee and Rotaru, 2020) and likely contributed to DIET in our experimental system. The low representation of methanogens in our communities overall may be attributed to the poor specificity of the universal 515F/806R primers towards archaeal sequences in general (Raymann et al., 2017). Due to constraints resulting from low DNA extraction yields from many of our samples, we were only able to re-sequence a subset of our samples using archaeal specific 519F/915R primers. With this primer pair, we were able to detect a greater presence of Methanobacteria in a few of our "No Mineral" treatment samples (T4S1 and T8S2), which is interesting as we did not detect any accumulation of methane in any cultures in this treatment group, consistent with the hypothesis that crystalline iron oxides are needed to facilitate DIET-mediated methanogenesis in our system. We detected some Methanosarcinia at higher relative abundances in only a few of our only a few a few of our "Hematite" treatment samples (T4SH1 and T8SH3, Fig. S5).

3.4 Effects of metabolism inhibitors on microbial communities

Parallel experiments using either BES or molybdate to inhibit methanogenesis and sulfate reduction respectively were conducted to determine the contribution of each metabolism to the syntrophic interactions occurring in our incubations. BES is an analog of coenzyme M and is known to disrupt methanogenesis by irreversibly binding to the active site of methyl coenzyme M reductase (Mcr), preventing the enzyme from catalyzing the reduction of methyl coenzyme M to methane (Goenrich et al., 2004). Our results are consistent with this knowledge, as methane accumulation did not occur in the headspace of our BES amended incubations. Trends in the production or consumption of all other compounds measured are similar to what was observed in the inhibitor free conditions (Fig. 1, plots S, SH, SF, SB, SHB, SHF). While the composition of the microbial communities incubated with BES appear similar to the uninhibited control experiments (see Fig. S6 for microbial community composition data grouped by inhibitor used), the differences between the structure of the BES treated communities were significantly different than the original inoculum, communities treated with molybdate, and communities that were left uninhibited (Pairwise PERMANOVA p-values <0.05 for all pairwise comparisons, Table S2). This is likely due to decreases in relative abundances of the Desulfitobacteriia collected day 36 (T4) and Day 87 (T4) and increases in the abundances of the Desulfomaculia increased during this period.

Molybdate is canonically known to selectively inhibit sulfate reduction metabolisms by targeting sulfate adenylyltranserase (Sat), an enzyme that uses ATP to activate inert sulfate ions, forming adenosine 5' phosphosulfate (APS)

https://doi.org/10.5194/bg-2023-174
Preprint. Discussion started: 29 September 2023

in the process. Upon binding to Sat's active site, molybdate converts to an unstable adenosine 5' molybdophosphate (APMo) product, also consuming ATP in the process. This depletion of ATP can rapidly decrease the cellular energy reserves, leading to overall inhibition in the organism(Taylor and Oremland, 1979). Given this, it is unsurprising that we observed little change in sulfate concentrations and no accumulation of sulfide over time in the molybdate treatments (Fig. 1, plots SM, SHM, SFM). We did, however, expect DIET between organisms with putative Fe reducing metabolisms and methanogens in the SHM incubations to still occur, as the addition of molybdate is not known to affect Fe reduction metabolic pathways. Methane was not produced in SHM incubations (Fig. 1).

Recent work revealed that a mutant strain of *Desulfovibrio vulgaris* Hildenborough lacking Sat was still inhibited by molybdate addition. Further investigation suggested that molybdate likely also targeted a protein containing a YcaO domain in this organism (Zane et al., 2020). While this YcaO-like protein has yet to be fully characterized in *D. vulgaris*, this protein superfamily is known for several critical functions, including azoline, macroamindine, and thioamide formation, catalysis of RimO-dependant methylthiolation, and biosynthesis of ribosomally synthesized and posttranslationally modified peptides (Burkhart et al., 2017). YcaO- like proteins can engage in phosphorylation reactions and contain an ATP binding motif that's highly conserved throughout the superfamily (Dunbar et al., 2014). Zane et al., posited in 2020 that molybdate is also a substrate for YcaO-like proteins, forming APMo upon phosphorylation, leading to a similar depletion of intracellular energy reserves as observed during Sat inhibition.

There are currently more than 17,000 proteins containing Ycao-like domains listed in the InterPro database (Accession no: IPR003776), spanning wide phylogenetic diversity within both bacteria and archaea. We searched this database and found Ycao-like domain containing proteins in several species representative of the genera enriched in our incubations that were either highly abundant or putatively have metabolisms that are relevant for our study. These genera include, *Lactobacillus, Lachnoclostrdium, Desulfosporosinus, Anaeromyxobacter, Sporomusa, Syntrophomonas, Methanosarcina, Methanobacterium*, and several members of the Anaerolineae (see Table S3 for list of species and Interpro accession numbers). It is possible that molybdate amendment to our incubations not only specifically inhibited sulfate reduction, but also inhibited the general physiology of many of the other organisms. The absence of methane production in SHM cultures could possibly be attributed to general inhibition of the Fe reducers and/or the methanogens, reducing the organisms' capabilities to perform DIET. We detected much less acid-extractable Fe(II) in our ferrihydrite treatments when molybdate was provided compared to molybdate free incubations (Fig. 1 and S7, panel SFM) and the lack of peaks associated with reduced ferrous iron in XANES analyses for sample SFM (Fig. 3A), providing further support for the inhibition of Fe reducing microbes via molybdate. Very little butyrate was consumed and much less acetate was produced in the molybdate treatments compared to the other conditions (Fig. 1, panels SM, SHM, and SFM), suggesting that many of the fermenters were inhibited by molybdate as well.

It is also worth noting that the concentration of molybdate used (10 mM) may have been high enough to impart global toxicity on several of the organisms, regardless of whether they express YcaO domain containing proteins. Recently, molybdates's IC50 for sulfide production by both a sulfate-reducing enrichment culture and model SRB *Desulfovibrio alaskensis* G20 were calculated to be 0.0069 mM and 0.089 mM, respectively. In addition, the IC50s for overall growth (as

https://doi.org/10.5194/bg-2023-174
Preprint. Discussion started: 29 September 2023

determined by OD 600 measurements) for this sulfidogenic enrichment culture and *D. alaskensis* G20 grown using pyruvate as an electron acceptor were 0.69 mM and 0.092 mM, respectively (Carlson et al., 2021). Since more than an order of magnitude more molybdate was used in our sediment incubations, it is possible that metabolic activity and growth of most organisms enriched in these cultures was arrested.

The composition of the microbial communities was also significantly affected by the addition of molybdate, as Bray-Curtis dissimilarity metrics indicated significant differences in composition of molybdate treated communities and the initial inoculum, communities where no inhibitors were added, and communities treated with BES (PERMANOVA p-values = 0.001 for all pairwise comparisons, Table S2, Fig. S8). Molybdate incubations were largely dominated by Clostridia. Desulfitobacteriia and Desulfotomaculia were still detected in samples collected at day 36 but decreased in abundance by day 87. While Methanobacteria were observed in several of the molybdate incubations, we were unable to detect the presence of Methanosarcinia. These differences in community composition in response to molybdate addition may also partially explain the lack of methane production in our SHM incubations, as the organisms most likely to engage in DIET were found in much lower abundances in these communities than in the incubations where no inhibitors were added.

3.5 Investigation of microbe-mineral interactions mechanisms

Possible mechanisms of microbe-mineral interactions that may explain observations from our incubations are presented in Fig 4. In all inhibitor-free conditions (Fig. 4A), the consumption of butyrate coincided with the reduction of sulfate by sulfate reducing bacteria. We observed the production of methane in incubations amended with hematite, presumably through DIET mechanisms between sulfate/Fe reducing microbes and methanogens. We did not observe methane production in incubations amended with ferrihydrite. Fe reducers enriched during these incubations were likely able to use the more reactive ferrihydrite as an electron acceptor, resulting in its reductive dissolution and subsequent release of Fe(II) (Figs. 1, 3A, and S2) previous studies (Tang et al., 2021).

Natural enrichment of several genera of Fe reducing microbes in our incubations made it challenging to specifically determine how much sulfate-reducing metabolisms contributed to DIET in the presence of hematite, a phenomenon that has already been well studied in sedimentary environments (Aromokeye et al., 2018, 2020; Rotaru et al., 2018; Zhang and Lu, 2016). In addition, members of enriched genera, including *Desulfispora, Desulfosporosinus*, and potentially organisms from Actinobacteria group OPB41, are known to engage in both sulfate and Fe reduction, further obscuring microbe-mineral interactions occurring within these incubations.

Molybdate was used to specifically inhibit sulfate-reducers to assess their contribution to methane production and DIET processes occurring in our system (Fig. 4B). However, we may have also inadvertently inhibited the general physiologies of Fe-reducers and many other microbes that we enriched, likely due to molybdate also targeting the ubiquitous biosynthesis proteins of the YcaO superfamily, leading to subsequent ATP depletion. In addition to lack of methane production as a result of DIET in our SHM conditions, there was an overall decrease in Fe reduction capacities in these cultures, indicated by lower accumulation of acid-extractable Fe(II) in SFM incubations compared to SF and SFB conditions (Fig. 1 and S7).

Interactions at the biotic/abiotic interface are complex in terrestrial subsurface environments and this study further elucidates these intricately linked processes by emphasizing the role that both microbes and minerals play in facilitating biogeochemical cycles. Our results highlight the direct influences mineralogy has on microbial biogeochemistry. We showed that methanogenesis can occur under sulfate replete conditions when crystalline Fe oxides are present to mediate DIET interactions between microbial partners. This study helps to explain the co-occurrence of sulfate reduction and methane production in other terrestrial subsurface environments rich in semiconducting Fe minerals.

Data Availability

The raw sequences analyzed for this study are available in the NCBI repository under BioProject PRJNA945499, BioSample Accession numbers SAMN33786795 through SAMN33786856.

Author Contributions

MY, and RC designed experiments. MY and KCG performed the incubation experiments. BE, MY, KCG, AB performed analyses. BE, AB, and SGD contributed to initial manuscript draft. BE, RC, MY, KC, SGD, TH reviewed and edited the manuscript.

Competing Interests

The authors declare that they have no conflict of interest.

Acknowledgements

This material by ENIGMA- Ecosystems and Networks Integrated with Genes and Molecular Assemblies (http://enigma.lbl.gov), a Science Focus Area Program at Lawrence Berkeley National Laboratory is based upon work supported by the U.S. Department of Energy, Office of Science, Office of Biological & Environmental Research under contract number DE-AC02-05CH11231.

Use of the Stanford Synchrotron Radiation Lightsource, SLAC National Accelerator Laboratory, is supported by the U.S. Department of Energy, Office of Science, Office of Basic Energy Sciences under Contract No. DE-AC02-76SF00515. The SSRL Structural Molecular Biology Program is supported by the DOE Office of Biological and Environmental Research, and by the National Institutes of Health, National Institute of General Medical Sciences (P30GM133894). The contents of this publication are solely the responsibility of the authors and do not necessarily represent the official views of NIGMS or NIH.

We thank Dr. Shwetha Acharya, Dr. Mingfei Chen, Dr. Judy Wall, Dr. Adam Arkin, Dr. Karrie Weber, and Grant Zane for their helpful discussion and feedback through the experiment. We thank Eunice Tsang for assistance with sampling

and ferrozine assays. We also thank Dr. Matthew Latimer for assistance during with the synchrotron during our beamtime session at SLAC.

References

Aromokeye, D. A., Richter-Heitmann, T., Oni, O. E., Kulkarni, A., Yin, X., Kasten, S., and Friedrich, M. W.: Temperature Controls Crystalline Iron Oxide Utilization by Microbial Communities in Methanic Ferruginous Marine Sediment Incubations, Frontiers in Microbiology, 9, 2018.

Aromokeye, D. A., Kulkarni, A. C., Elvert, M., Wegener, G., Henkel, S., Coffinet, S., Eickhorst, T., Oni, O. E., Richter-Heitmann, T., Schnakenberg, A., Taubner, H., Wunder, L., Yin, X., Zhu, Q., Hinrichs, K.-U., Kasten, S., and Friedrich, M. W.: Rates and Microbial Players of Iron-Driven Anaerobic Oxidation of Methane in Methanic Marine Sediments, Frontiers in Microbiology, 10, 2020.

Benner, S. G., Hansel, C. M., Wielinga, B. W., Barber, T. M., and Fendorf, S.: Reductive Dissolution and Biomineralization of Iron Hydroxide under Dynamic Flow Conditions, Environ. Sci. Technol., 36, 1705–1711, https://doi.org/10.1021/es0156441, 2002.

Bird, J. T., Tague, E. D., Zinke, L., Schmidt, J. M., Steen, A. D., Reese, B., Marshall, I. P. G., Webster, G., Weightman, A., Castro, H. F., Campagna, S. R., and Lloyd, K. G.: Uncultured Microbial Phyla Suggest Mechanisms for Multi-Thousand-Year Subsistence in Baltic Sea Sediments, mBio, 10, e02376-18, https://doi.org/10.1128/mBio.02376-18, 2019.

Bolyen, E., Rideout, J. R., Dillon, M. R., Bokulich, N. A., Abnet, C. C., Al-Ghalith, G. A., Alexander, H., Alm, E. J., Arumugam, M., Asnicar, F., Bai, Y., Bisanz, J. E., Bittinger, K., Brejnrod, A., Brislawn, C. J., Brown, C. T., Callahan, B. J., Caraballo-Rodríguez, A. M., Chase, J., Cope, E. K., Da Silva, R., Diener, C., Dorrestein, P. C., Douglas, G. M., Durall, D. M., Duvallet, C., Edwardson, C. F., Ernst, M., Estaki, M., Fouquier, J., Gauglitz, J. M., Gibbons, S. M., Gibson, D. L., Gonzalez, A., Gorlick, K., Guo, J., Hillmann, B., Holmes, S., Holste, H., Huttenhower, C., Huttley, G. A., Janssen, S., Jarmusch, A. K., Jiang, L., Kaehler, B. D., Kang, K. B., Keefe, C. R., Keim, P., Kelley, S. T., Knights, D., Koester, I., Kosciolek, T., Kreps, J., Langille, M. G. I., Lee, J., Ley, R., Liu, Y.-X., Loftfield, E., Lozupone, C., Maher, M., Marotz, C., Martin, B. D., McDonald, D., McIver, L. J., Melnik, A. V., Metcalf, J. L., Morgan, S. C., Morton, J. T., Naimey, A. T., Navas-Molina, J. A., Nothias, L. F., Orchanian, S. B., Pearson, T., Peoples, S. L., Petras, D., Preuss, M. L., Pruesse, E., Rasmussen, L. B., Rivers, A., Robeson, M. S., Rosenthal, P., Segata, N., Shaffer, M., Shiffer, A., Sinha, R., Song, S. J., Spear, J. R., Swafford, A. D., Thompson, L. R., Torres, P. J., Trinh, P., Tripathi, A., Turnbaugh, P. J., Ul-Hasan, S., van der Hooft, J. J. J., Vargas, F., Vázquez-Baeza, Y., Vogtmann, E., von Hippel, M., et al.: Reproducible, interactive, scalable and extensible microbiome data science using QIIME 2, Nature Biotechnology, 37, 852–857, https://doi.org/10.1038/s41587-019-0209-9, 2019.

Boone, D. R.: *Methanobacterium*, in: Bergey's Manual of Systematics of Archaea and Bacteria, edited by: Whitman, W. B., Rainey, F., Kämpfer, P., Trujillo, M., Chun, J., DeVos, P., Hedlund, B., and Dedysh, S., Wiley, 1–8, https://doi.org/10.1002/9781118960608.gbm00495, 2015.

Brauman, A., Muller, J. A., Garcia, J.-L., Brune, A., and Schink, B.: Fermentative degradation of 3-hydroxybenzoate in pure culture by a novel strictly anaerobic bacterium, Sporotomaculum hydroxybenzoicum gen. nov., sp. nov., International Journal of Systematic Bacteriology, 48, 215–221, https://doi.org/10.1099/00207713-48-1-215, 1998.

Breznak, J. A. and Blum, J. S.: Mixotrophy in the termite gut acetogen, Sporomusa termitida, Arch. Microbiol., 156, 105–110, https://doi.org/10.1007/BF00290981, 1991.

Burkhart, B. J., Schwalen, C. J., Mann, G., Naismith, J. H., and Mitchell, D. A.: YcaO-Dependent Posttranslational Amide Activation: Biosynthesis, Structure, and Function, Chem. Rev., 117, 5389–5456, https://doi.org/10.1021/acs.chemrev.6b00623, 2017.

Caporaso, J. G., Lauber, C. L., Walters, W. A., Berg-Lyons, D., Lozupone, C. A., Turnbaugh, P. J., Fierer, N., and Knight, R.: Global patterns of 16S rRNA diversity at a depth of millions of sequences per sample, Proceedings of the National Academy of Sciences, 108, 4516–4522, https://doi.org/10.1073/pnas.1000080107, 2011.

Carlson, H. K., Youngblut, M. D., Redford, S. A., Williamson, A. J., and Coates, J. D.: Sulfate adenylyl transferase kinetics and mechanisms of metabolic inhibitors of microbial sulfate respiration, ISME COMMUN., 1, 67, https://doi.org/10.1038/s43705-021-00069-1, 2021.

Casamayor, E. O., Massana, R., Benlloch, S., Øvreås, L., Díez, B., Goddard, V. J., Gasol, J. M., Joint, I., Rodríguez-Valera, F., and Pedrós-Alió, C.: Changes in archaeal, bacterial and eukaryal assemblages along a salinity gradient by comparison of genetic fingerprinting methods in a multipond solar saltern, Environmental Microbiology, 4, 338–348, https://doi.org/10.1046/j.1462-2920.2002.00297.x, 2002.

Claypool, G. E. and Kaplan, I. R.: The Origin and Distribution of Methane in Marine Sediments, in: Natural Gases in Marine Sediments, edited by: Kaplan, I. R., Springer US, Boston, MA, 99–139, https://doi.org/10.1007/978-1-4684-2757-8_8, 1974.

Cline, J. D.: Spectrophotometric Determination of Hydrogen Sulfide in Natural Waters, Limnology and Oceanography, 14, 454–458, https://doi.org/10.4319/lo.1969.14.3.0454, 1969.

Cornell, R. M. and Schwertmann, U.: The iron oxides: Structure, properties, reactions, occurrence and uses, Weinheim: Wiley-vch., 664, https://doi.org/10.1016/S0010-938X(97)00096-6, 2003.

Davis, N. M., Proctor, D. M., Holmes, S. P., Relman, D. A., and Callahan, B. J.: Simple statistical identification and removal of contaminant sequences in marker-gene and metagenomics data, Microbiome, 6, https://doi.org/10.1186/s40168-018-0605-2, 2018.

Dixon, P.: VEGAN, a package of R functions for community ecology, Journal of Vegetation Science, 14, 927–930, https://doi.org/10.1111/j.1654-1103.2003.tb02228.x, 2003.

Drake, H. L., Daniel, S. L., Küsel, K., Matthies, C., Kuhner, C., and Braus-Stromeyer, S.: Acetogenic bacteria: what are the *in situ* consequences of their diverse metabolic versatilities?, BioFactors, 6, 13–24, https://doi.org/10.1002/biof.5520060103, 1997.

Dunbar, K. L., Chekan, J. R., Cox, C. L., Burkhart, B. J., Nair, S. K., and Mitchell, D. A.: Discovery of a new ATP-binding motif involved in peptidic azoline biosynthesis, Nat Chem Biol, 10, 823–829, https://doi.org/10.1038/nchembio.1608, 2014.

Dworkin, M., Falkow, S., Rosenberg, E., Schleifer, K.-H., and Stackebrandt, E. (Eds.): The Prokaryotes, Springer New York, New York, NY, https://doi.org/10.1007/0-387-30742-7, 2006.

Goenrich, M., Mahlert, F., Duin, E. C., Bauer, C., Jaun, B., and Thauer, R. K.: Probing the reactivity of Ni in the active site of methyl-coenzyme M reductase with substrate analogues, J Biol Inorg Chem, 9, 691–705, https://doi.org/10.1007/s00775-004-0552-1, 2004.

He, Q. and Sanford, R. A.: Characterization of Fe(III) Reduction by Chlororespiring Anaeromxyobacter dehalogenans, Appl Environ Microbiol, 69, 2712–2718, https://doi.org/10.1128/AEM.69.5.2712-2718.2003, 2003.

Herfort, L., Kim, J.-H., Coolen, M. J. L., Abbas, B., Schouten, S., Herndl, G. J., and Damsté, J. S. S.: Diversity of Archaea and detection of crenarchaeotal amoA genes in the rivers Rhine and Têt, Aquatic Microbial Ecology, 55, 189–201, https://doi.org/10.3354/ame01294, 2009.

Hippe, H. and Stackebrandt, E.: *Desulfosporosinus*, in: Bergey's Manual of Systematics of Archaea and Bacteria, edited by: Whitman, W. B., Rainey, F., Kämpfer, P., Trujillo, M., Chun, J., DeVos, P., Hedlund, B., and Dedysh, S., Wiley, 1–10, https://doi.org/10.1002/9781118960608.gbm00660, 2015.

Imachi, H., Sakai, S., Lipp, J. S., Miyazaki, M., Saito, Y., Yamanaka, Y., Hinrichs, K.-U., Inagaki, F., and Takai, K.: Pelolinea submarina gen. nov., sp. nov., an anaerobic, filamentous bacterium of the phylum Chloroflexi isolated from subseafloor sediment, International Journal of Systematic and Evolutionary Microbiology, 64, 812–818, https://doi.org/10.1099/ijs.0.057547-0, 2014.

Jørgensen, B. B. and Kasten, S.: Sulfur Cycling and Methane Oxidation, in: Marine Geochemistry, edited by: Schulz, H. D. and Zabel, M., Springer, Berlin, Heidelberg, 271–309, https://doi.org/10.1007/3-540-32144-6_8, 2006.

Jørgensen, B. B., Findlay, A. J., and Pellerin, A.: The Biogeochemical Sulfur Cycle of Marine Sediments, Frontiers in Microbiology, 10, 2019.

Kaksonen, A. H., Spring, S., Schumann, P., Kroppenstedt, R. M., and Puhakka, J. A.: Desulfurispora thermophila gen. nov., sp. nov., a thermophilic, spore-forming sulfate-reducer isolated from a sulfidogenic fluidized-bed reactor, International Journal of Systematic and Evolutionary Microbiology, 57, 1089–1094, https://doi.org/10.1099/ijs.0.64593-0, 2007.

Kato, S., Hashimoto, K., and Watanabe, K.: Microbial interspecies electron transfer via electric currents through conductive minerals, Proceedings of the National Academy of Sciences, 109, 10042–10046, https://doi.org/10.1073/pnas.1117592109, 2012.

Khomyakova, M. A., Zavarzina, D. G., Merkel, A. Y., Klyukina, A. A., Pikhtereva, V. A., Gavrilov, S. N., and Slobodkin, A. I.: The first cultivated representatives of the actinobacterial lineage OPB41 isolated from subsurface environments constitute a novel order Anaerosomatales, Front. Microbiol., 13, 1047580, https://doi.org/10.3389/fmicb.2022.1047580, 2022.

Kim, J. R., Beecroft, N. J., Varcoe, J. R., Dinsdale, R. M., Guwy, A. J., Slade, R. C. T., Thumser, A., Avignone-Rossa, C., and Premier, G. C.: Spatiotemporal development of the bacterial community in a tubular longitudinal microbial fuel cell, Appl Microbiol Biotechnol, 90, 1179–1191, https://doi.org/10.1007/s00253-011-3181-y, 2011.

Kleber, M., Eusterhues, K., Keiluweit, M., Mikutta, C., Mikutta, R., and Nico, P. S.: Mineral–Organic Associations: Formation, Properties, and Relevance in Soil Environments, in: Advances in Agronomy, vol. 130, Elsevier, 1–140, https://doi.org/10.1016/bs.agron.2014.10.005, 2015.

Koster, I., Rinzema, A., Devegt, A., and Lettinga, G.: Sulfide inhibition of the methanogenic activity of granular sludge at various pH-levels, Water Research, 20, 1561–1567, https://doi.org/10.1016/0043-1354(86)90121-1, 1986.

Kristjansson, J. K., Schönheit, P., and Thauer, R. K.: Different Ks values for hydrogen of methanogenic bacteria and sulfate reducing bacteria: An explanation for the apparent inhibition of methanogenesis by sulfate, Arch. Microbiol., 131, 278–282, https://doi.org/10.1007/BF00405893, 1982.

Li, Y.-L., Vali, H., Yang, J., Phelps, T. J., and Zhang, C. L.: Reduction of Iron Oxides Enhanced by a Sulfate-Reducing Bacterium and Biogenic H2S, Geomicrobiology Journal, 23, 103–117, https://doi.org/10.1080/01490450500533965, 2006.

Melton, E. D., Swanner, E. D., Behrens, S., Schmidt, C., and Kappler, A.: The interplay of microbially mediated and abiotic reactions in the biogeochemical Fe cycle, Nat Rev Microbiol, 12, 797–808, https://doi.org/10.1038/nrmicro3347, 2014.

Michael Madigan, Bender, K., Buckley, D., Sattley, W. M., and Stahl, D.: Brock Biology of Microorganisms, 15th ed., Pearson, New York, NY, USA, 2019.

Mikutta, C., Mikutta, R., Bonneville, S., Wagner, F., Voegelin, A., Christl, I., and Kretzschmar, R.: Synthetic coprecipitates of exopolysaccharides and ferrihydrite. Part I: Characterization, Geochimica et Cosmochimica Acta, 72, 1111–1127, https://doi.org/10.1016/j.gca.2007.11.035, 2008.

Moon, J.-W., Paradis, C. J., Joyner, D. C., von Netzer, F., Majumder, E. L., Dixon, E. R., Podar, M., Ge, X., Walian, P. J., Smith, H. J., Wu, X., Zane, G. M., Walker, K. F., Thorgersen, M. P., Poole II, F. L., Lui, L. M., Adams, B. G., De León, K. B., Brewer, S. S., Williams, D. E., Lowe, K. A., Rodriguez, M., Mehlhorn, T. L., Pfiffner, S. M., Chakraborty, R., Arkin, A. P., Wall, J. D., Fields, M. W., Adams, M. W. W., Stahl, D. A., Elias, D. A., and Hazen, T. C.: Characterization of subsurface media from locations up- and down-gradient of a uranium-contaminated aquifer, Chemosphere, 255, 126951, https://doi.org/10.1016/j.chemosphere.2020.126951, 2020.

Neal, A. L., Techkarnjanaruk, S., Dohnalkova, A., McCready, D., Peyton, B. M., and Geesey, G. G.: Iron sulfides and sulfur species produced at hematite surfaces in the presence of sulfate-reducing bacteria11Associate editor: D. J. Wesolowski, Geochimica et Cosmochimica Acta, 65, 223–235, https://doi.org/10.1016/S0016-7037(00)00537-8, 2001.

Nozhevnikova, A. N., Russkova, Yu. I., Litti, Yu. V., Parshina, S. N., Zhuravleva, E. A., and Nikitina, A. A.: Syntrophy and Interspecies Electron Transfer in Methanogenic Microbial Communities, Microbiology, 89, 129–147, https://doi.org/10.1134/S0026261720020101, 2020.

O'Day, P. A., Rivera, N., Root, R., and Carroll, S. A.: X-ray absorption spectroscopic study of Fe reference compounds for the analysis of natural sediments, American Mineralogist, 89, 572–585, https://doi.org/10.2138/am-2004-0412, 2004.

Oremland, R. S. and Polcin, S.: Methanogenesis and Sulfate Reduction: Competitive and Noncompetitive Substrates in Estuarine Sediments, Applied and Environmental Microbiology, https://doi.org/10.1128/aem.44.6.1270-1276.1982, 1982.

Owusu-Agyeman, I., Plaza, E., and Cetecioglu, Z.: Long-term alkaline volatile fatty acids production from waste streams: Impact of pH and dominance of Dysgonomonadaceae, Bioresource Technology, 346, 126621, https://doi.org/10.1016/j.biortech.2021.126621, 2022.

Ozuolmez, D., Moore, E. K., Hopmans, E. C., Sinninghe Damsté, J. S., Stams, A. J. M., and Plugge, C. M.: Butyrate Conversion by Sulfate-Reducing and Methanogenic Communities from Anoxic Sediments of Aarhus Bay, Denmark, Microorganisms, 8, 606, https://doi.org/10.3390/microorganisms8040606, 2020.

Park, J.-H., Kang, H.-J., Park, K.-H., and Park, H.-D.: Direct interspecies electron transfer via conductive materials: A perspective for anaerobic digestion applications, Bioresource Technology, 254, 300–311, https://doi.org/10.1016/j.biortech.2018.01.095, 2018.

Parte, A., Krieg, N. R., Ludwig, W., Whitman, W. B., Hedlund, B. P., Paster, B. J., Staley, J. T., Ward, N., and Brown, D.: Bergey's Manual of Systematic Bacteriology: Volume 4: The Bacteroidetes, Spirochaetes, Tenericutes (Mollicutes), Acidobacteria, Fibrobacteres, Fusobacteria, Dictyoglomi, Gemmatimonadetes, Lentisphaerae, Verrucomicrobia, Chlamydiae, and Planctomycetes, Springer Science & Business Media, 966 pp., 2011.

Petrie, L., North, N. N., Dollhopf, S. L., Balkwill, D. L., and Kostka, J. E.: Enumeration and Characterization of Iron(III)-ReducingMicrobial Communities from Acidic Subsurface Sediments ContaminatedwithUranium(VI), Appl Environ Microbiol, 69, 7467–7479, https://doi.org/10.1128/AEM.69.12.7467-7479.2003, 2003.

Poulton, S. W.: Sulfide oxidation and iron dissolution kinetics during the reaction of dissolved sulfide with ferrihydrite, Chemical Geology, 202, 79–94, https://doi.org/10.1016/S0009-2541(03)00237-7, 2003.

Prietzel, J., Botzaki, A., Tyufekchieva, N., Brettholle, M., Thieme, J., and Klysubun, W.: Sulfur Speciation in Soil by S K-Edge XANES Spectroscopy: Comparison of Spectral Deconvolution and Linear Combination Fitting, Environ. Sci. Technol., 45, 2878–2886, https://doi.org/10.1021/es102180a, 2011.

Pyzik, A. J. and Sommer, S. E.: Sedimentary iron monosulfides: Kinetics and mechanism of formation, Geochimica et Cosmochimica Acta, 45, 687–698, https://doi.org/10.1016/0016-7037(81)90042-9, 1981.

Ravel, B. and Newville, M.: ATHENA, ARTEMIS, HEPHAESTUS: data analysis for X-ray absorption spectroscopy using IFEFFIT, J Synchrotron Rad, 12, 537–541, https://doi.org/10.1107/S0909049505012719, 2005.

Raymann, K., Moeller, A. H., Goodman, A. L., and Ochman, H.: Unexplored Archaeal Diversity in the Great Ape Gut Microbiome, mSphere, 2, e00026-17, https://doi.org/10.1128/mSphere.00026-17, 2017.

Rotaru, A.-E., Calabrese, F., Stryhanyuk, H., Musat, F., Shrestha, P. M., Weber, H. S., Snoeyenbos-West, O. L. O., Hall, P. O. J., Richnow, H. H., Musat, N., and Thamdrup, B.: Conductive Particles Enable Syntrophic Acetate Oxidation between Geobacter and Methanosarcina from Coastal Sediments, mBio, 9, e00226-18, https://doi.org/10.1128/mBio.00226-18, 2018.

Rowe, A. R., Xu, S., Gardel, E., Bose, A., Girguis, P., Amend, J. P., and El-Naggar, M. Y.: Methane-Linked Mechanisms of Electron Uptake from Cathodes by Methanosarcina barkeri, mBio, 10, e02448-18, https://doi.org/10.1128/mBio.02448-18, 2019.

Satinover, S. J., Rodriguez, M., Campa, M. F., Hazen, T. C., and Borole, A. P.: Performance and community structure dynamics of microbial electrolysis cells operated on multiple complex feedstocks, Biotechnol Biofuels, 13, 169, https://doi.org/10.1186/s13068-020-01803-y, 2020.

Schönheit, P., Kristjansson, J. K., and Thauer, R. K.: Kinetic mechanism for the ability of sulfate reducers to out-compete methanogens for acetate, Arch. Microbiol., 132, 285–288, https://doi.org/10.1007/BF00407967, 1982.

Schwertmann, U.: Solubility and dissolution of iron oxides, Pland and soil, 130, 1–25, 1991.

Stookey, L. L.: Ferrozine---a new spectrophotometric reagent for iron, Anal. Chem., 42, 779–781, https://doi.org/10.1021/ac60289a016, 1970.

Struchtemeyer, C. G., Duncan, K. E., and McInerney, M. J.: Evidence for syntrophic butyrate metabolism under sulfate-reducing conditions in a hydrocarbon-contaminated aquifer, FEMS Microbiology Ecology, 76, 289–300, https://doi.org/10.1111/j.1574-6941.2011.01046.x, 2011.

Tang, Y., Li, Y., Zhang, M., Xiong, P., Liu, L., Bao, Y., and Zhao, Z.: Link between characteristics of Fe(III) oxides and critical role in enhancing anaerobic methanogenic degradation of complex organic compounds, Environmental Research, 194, 110498, https://doi.org/10.1016/j.envres.2020.110498, 2021.

Taylor, B. F. and Oremland, R. S.: Depletion of adenosine triphosphate inDesulfovibrio by oxyanions of group VI elements, Current Microbiology, 3, 101–103, https://doi.org/10.1007/BF02602440, 1979.

Thauer, R. K., Stackebrandt, E., and Hamilton, W. A.: Energy metabolism and phylogenetic diversity of sulphate-reducing bacteria, in: Sulphate-Reducing Bacteria: Environmental and Engineered Systems, edited by: Barton, L. L. and Hamilton, W. A., Cambridge University Press, Cambridge, 1–38, https://doi.org/10.1017/CBO9780511541490.002, 2007.

Tremblay, P.-L. and Zhang, T.: Electrifying microbes for the production of chemicals, Front. Microbiol., 6, https://doi.org/10.3389/fmicb.2015.00201, 2015.

Ueki, A.: Paludibacter propionicigenes gen. nov., sp. nov., a novel strictly anaerobic, Gram-negative, propionate-producing bacterium isolated from plant residue in irrigated rice-field soil in Japan, International Journal Of Systematic And Evolutionary Microbiology, 56, 39–44, https://doi.org/10.1099/ijs.0.63896-0, 2006.

Watanabe, M., Fukui, M., and Kuever, J.: *D esulfallaceae* fam. nov., in: Bergey's Manual of Systematics of Archaea and Bacteria, edited by: Whitman, W. B., Rainey, F., Kämpfer, P., Trujillo, M., Chun, J., DeVos, P., Hedlund, B., and Dedysh, S., Wiley, 1–3, https://doi.org/10.1002/9781118960608.fbm00343, 2020.

Watson, D. B., Kostka, J. E., Fields, M. W., and Jardine, P. M.: The Oak Ridge Field Research Center Conceptual Model, 2004.

Weihe, S. H. C., Mangayayam, M., Sand, K. K., and Tobler, D. J.: Hematite Crystallization in the Presence of Organic Matter: Impact on Crystal Properties and Bacterial Dissolution, ACS Earth Space Chem., 3, 510–518, https://doi.org/10.1021/acsearthspacechem.8b00166, 2019.

Wen, Y., Xiao, J., Liu, F., Goodman, B. A., Li, W., Jia, Z., Ran, W., Zhang, R., Shen, Q., and Yu, G.: Contrasting effects of inorganic and organic fertilisation regimes on shifts in Fe redox bacterial communities in red soils, Soil Biology and Biochemistry, 117, 56–67, https://doi.org/10.1016/j.soilbio.2017.11.003, 2018.

Wu, X., Spencer, S., Gushgari-Doyle, S., Yee, M. O., Voriskova, J., Li, Y., Alm, E. J., and Chakraborty, R.: Culturing of "Unculturable" Subsurface Microbes: Natural Organic Carbon Source Fuels the Growth of Diverse and Distinct Bacteria From Groundwater, Frontiers in Microbiology, 11, 2020.

Xu, Y. and Schoonen, M. A. A.: The absolute energy positions of conduction and valence bands of selected semiconducting minerals, American Mineralogist, 85, 543–556, https://doi.org/10.2138/am-2000-0416, 2000.

Yamada, T., Sekiguchi, Y., Hanada, S., Imachi, H., Ohashi, A., Harada, H., and Kamagata, Y. 2006: Anaerolinea thermolimosa sp. nov., Levilinea saccharolytica gen. nov., sp. nov. and Leptolinea tardivitalis gen. nov., sp. nov., novel filamentous anaerobes, and description of the new classes Anaerolineae classis nov. and Caldilineae classis nov. in the bacterial phylum Chloroflexi, International Journal of Systematic and Evolutionary Microbiology, 56, 1331–1340, https://doi.org/10.1099/ijs.0.64169-0, 2006.

Yao, W. and Millero, F. J.: Oxidation of hydrogen sulfide by hydrous Fe(III) oxides in seawater, Marine Chemistry, 52, 1–16, https://doi.org/10.1016/0304-4203(95)00072-0, 1996.

Yee, M. O. and Rotaru, A.-E.: Extracellular electron uptake in Methanosarcinales is independent of multiheme c-type cytochromes, Sci Rep, 10, 372, https://doi.org/10.1038/s41598-019-57206-z, 2020.

Yee, M. O., Snoeyenbos-West, O. L., Thamdrup, B., Ottosen, L. D. M., and Rotaru, A.-E.: Extracellular Electron Uptake by Two Methanosarcina Species, Frontiers in Energy Research, 7, 2019.

Yutin, N. and Galperin, M. Y.: A genomic update on clostridial phylogeny: Gram-negative spore formers and other misplaced clostridia: Genomics update, Environ Microbiol, https://doi.org/10.1111/1462-2920.12173, 2013.

https://doi.org/10.5194/bg-2023-174
Preprint. Discussion started: 29 September 2023

Zane, G. M., Wall, J. D., and De León, K. B.: Novel Mode of Molybdate Inhibition of Desulfovibrio vulgaris Hildenborough, Front. Microbiol., 11, 610455, https://doi.org/10.3389/fmicb.2020.610455, 2020.

Zhang, F., Battaglia-Brunet, F., Hellal, J., Joulian, C., Gautret, P., and Motelica-Heino, M.: Impact of Fe(III) (Oxyhydr)oxides Mineralogy on Iron Solubilization and Associated Microbial Communities, Frontiers in Microbiology, 11, 2020.

Zhang, J. and Lu, Y.: Conductive Fe3O4 Nanoparticles Accelerate Syntrophic Methane Production from Butyrate Oxidation in Two Different Lake Sediments, Frontiers in Microbiology, 7, 2016.

Zhou, S., Xu, J., Yang, G., and Zhuang, L.: Methanogenesis affected by the co-occurrence of iron(III) oxides and humic substances, FEMS Microbiology Ecology, 88, 107–120, https://doi.org/10.1111/1574-6941.12274, 2014.

Table 1. Description of biotic incubation conditions.

Experimental Acronym	Mineral Used	Inhibitor Used	Mechanism Evaluated

https://doi.org/10.5194/bg-2023-174
Preprint. Discussion started: 29 September 2023

S	None	None	Syntrophic butyrate degradation
SH	Hematite	None	
SF	Ferrihydrite	None	
SB	None	BES	5 mM BES added to inhibit methanogenesis; Syntropic butyrate degradation
SHB	Hematite	BES	
SFB	Ferrihydrite	BES	
SM	None	Molybdate	10 mM molybdate added to inhibit sulfate reduction; Syntrophic butyrate degradation
SHM	Hematite	Molybdate	
SFM	Ferrihydrite	Molybdate	

https://doi.org/10.5194/bg-2023-174
Preprint. Discussion started: 29 September 2023

Table 2. Description of abiotic incubation conditions and acronyms used to describe treatments.

Experimental Acronym	Mineral Used	Mechanism Evaluated
C	None	No microbial inoculum
CH	Hematite	
CF	Ferrihydrite	
CS	None	No microbial inoculum; 10 mM sulfide added to simulate sulfate reduction
CHS	Hematite	
CFS	Ferrihydrite	

https://doi.org/10.5194/bg-2023-174
Preprint. Discussion started: 29 September 2023

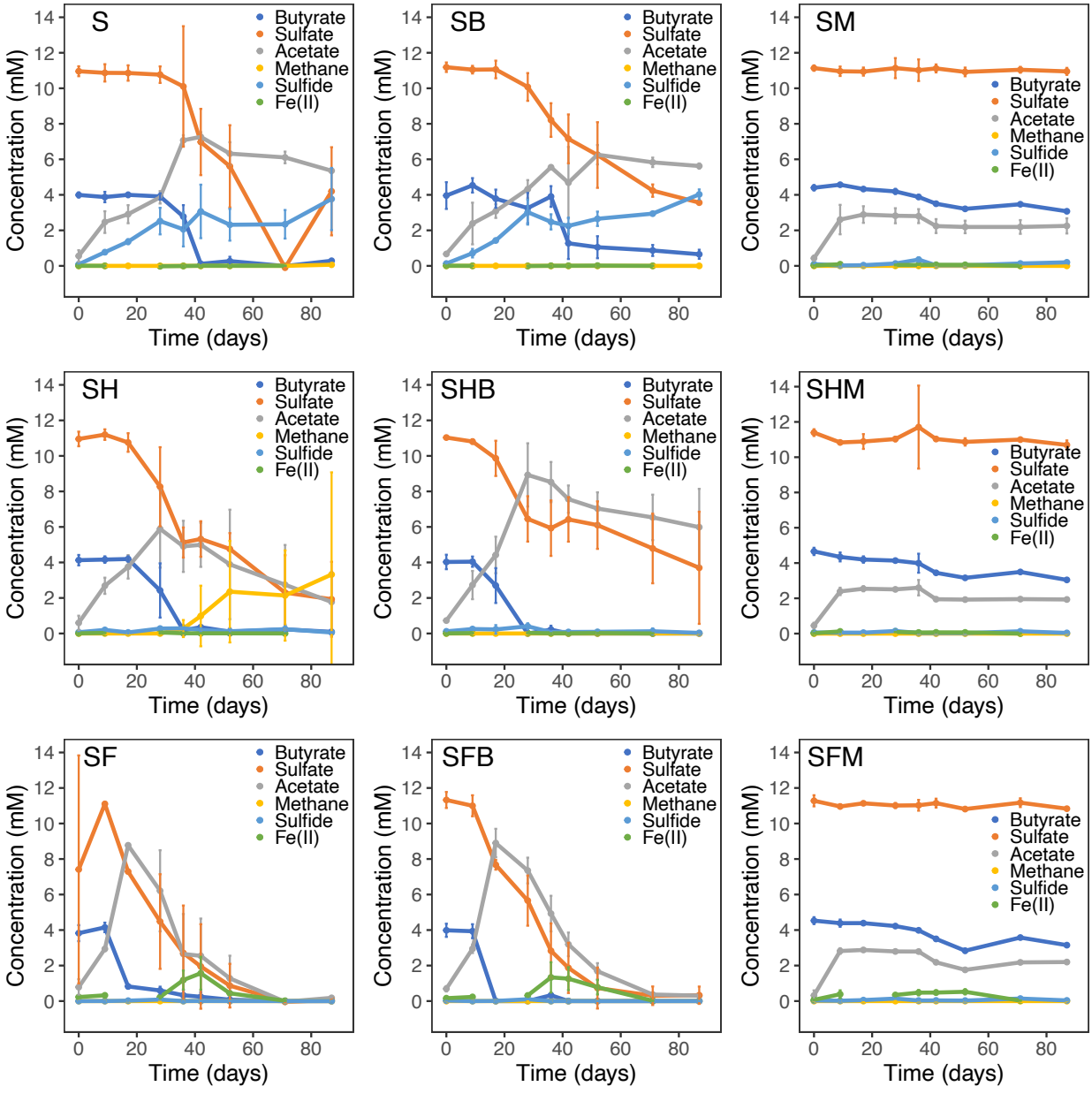

Figure 1. Aqueous concentrations (mM) of sulfate, sulfide, butyrate, acetate, ferrous iron, and methane over the duration of the 87 day experiment for the nine conditions. Error bars represent one standard deviation of experimental triplicates.

https://doi.org/10.5194/bg-2023-174
Preprint. Discussion started: 29 September 2023

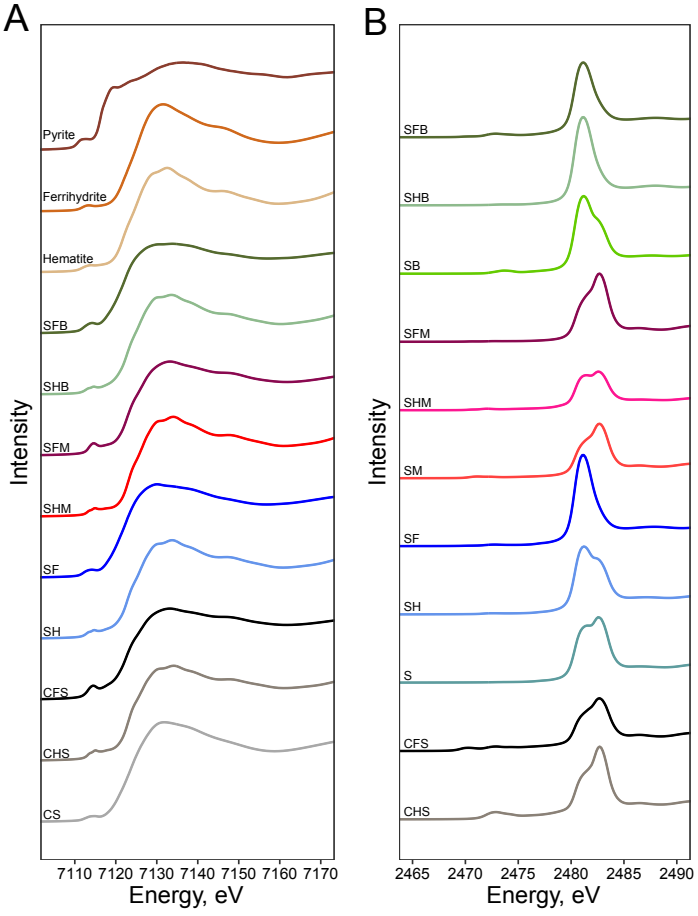

Figure 2. Normalized Fe and S K-edge x-ray absorption near-edge spectroscopy (XANES) data (Panels A and B respectively) in samples collected after biotic incubations with either hematite (SH) or ferrihydrite (SF) compared with samples from abiotic control incubations using added sulfide with either hematite (CHS) or ferrihydrite (CFS). Fe K-edge XANES spectra from pure hematite, ferrihydrite (Fe in $^{3+}$ oxidation state) and pyrite (Fe in $^{2+}$ oxidation state) are included in Panel A to compare peak positions for reference oxidation states.

https://doi.org/10.5194/bg-2023-174
Preprint. Discussion started: 29 September 2023

Biogeosciences Discussions
Open Access
EGU

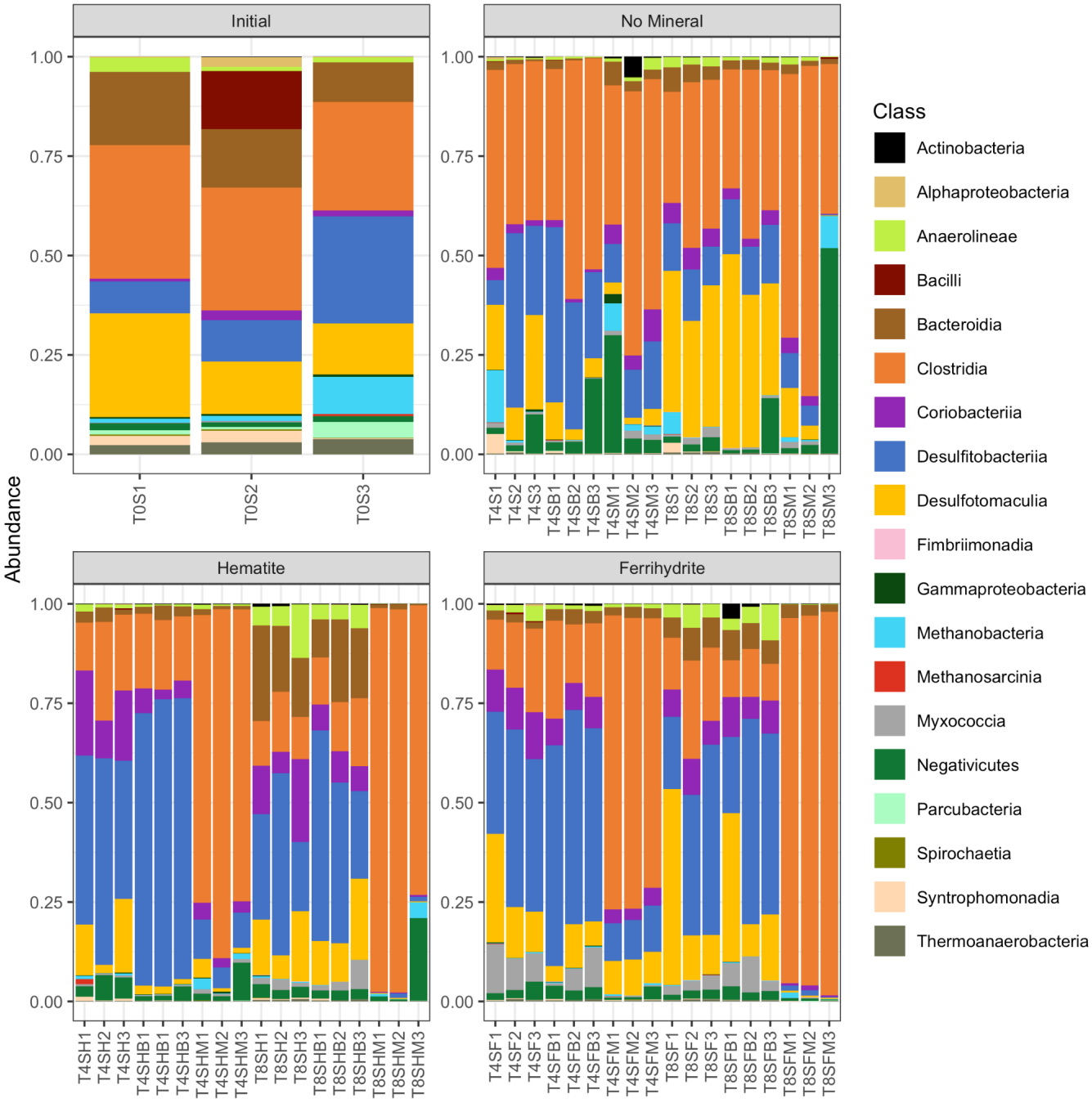

Figure 3. Microbial community composition data based on 16S rRNA phylogenetics. Samples labeled with T0, T4, or T8 were collected at Days 0, 36, or 87, respectively. Bar plots were grouped according to the mineral used during the incubation. DNA was extracted and sequenced for each experimental triplicate.

https://doi.org/10.5194/bg-2023-174
Preprint. Discussion started: 29 September 2023

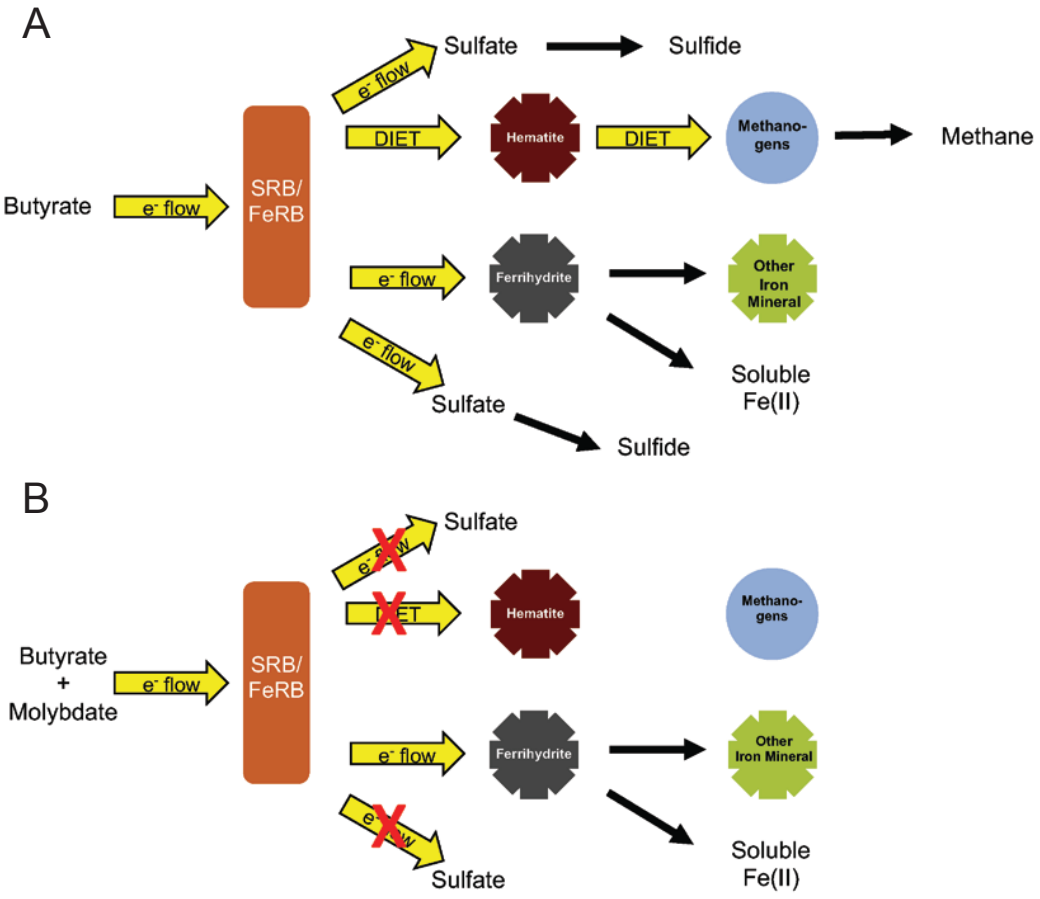

Figure 4. Proposed mechanism of microbe-mineral interactions in our system. A) Under uninhibited conditions, SRB and fermenters catalyze both the conversion of butyrate to acetate as well as the conversion of acetate to CO_2 and H_2. Iron reducing bacteria can utilize acetate, H_2, CO_2, or other organic substrates produced in the cultures to either reduce ferrihydrite or engage in EET transfer electrons to hematite. Methanogens in hematite amended cultures likely use electrons transferred to hematite from iron reducers to fix CO_2 into methane.